

Measuring a Parity Violation Signature in the Early Universe via Ground-based Laser Interferometers

Naoki Seto^{1,2} and Atsushi Taruya³

¹*National Astronomical Observatory, 2-21-1 Osawa, Mitaka, Tokyo, 181-8588, Japan*

²*Department of Physics and Astronomy, 4186 Frederick Reines Hall, University of California, Irvine, CA 92697*

³*Research Center for the Early Universe, School of Science,
The University of Tokyo, Tokyo 113-0033, Japan*

(Dated: October 29, 2018)

We show that pairs of widely separated interferometers are advantageous for measuring the Stokes parameter V of a stochastic background of gravitational waves. This parameter characterizes asymmetry of amplitudes of right- and left-handed waves and generation of the asymmetry is closely related to parity violation in the early universe. The advantageous pairs include LIGO (Livingston)-LCGT and AIGO-Virgo that are relatively insensitive to Ω_{GW} (the simple intensity of the background). Using at least three detectors, information of the intensity Ω_{GW} and the degree of asymmetry V can be separately measured.

I. INTRODUCTION

Stochastic background of gravitational waves is one of the most important targets for gravitational wave astronomy. In the last decade, the detection threshold for the background has been rapidly improved around $\sim 100\text{Hz}$ by continuous upgrades of ground-based interferometers [1]. This trend will be continued with advent of next-generation interferometers currently planned worldwide, such as advanced LIGO [2] and LCGT [3]. Due to the weakness of gravitational interaction, our universe is transparent to the background up to very early epoch, and we might uncover interesting nature of the universe at extremely high-energy scales, through observational studies of the stochastic background. To extract the information as much as possible, we need to characterize the background efficiently in a model independent manner, and investigation beyond simple spectral analysis might yield a great discovery. In this respect, circular polarization degree, which describes the asymmetry between the amplitudes of right- and left-handed waves, may be a fundamental characteristic of the background to probe the early universe. Because the parity transformation relates these two polarization modes, the asymmetry in the stochastic gravitational waves directly reflects a parity violation in the early universe, for instance, generated through the gravitational Chern-Simons term (e.g., [4]). In other words, one can detect a signature of parity violation by measuring the circular polarization degree of a gravitational wave background. Since the observed universe is highly isotropic and homogeneous, we shall focus on the monopole component of the circular polarization as our primary target, and report principle aspects for its measurement with a network of ground-based interferometers (see [5, 6] for CMB polarization and [7] for space missions).

II. CIRCULAR POLARIZATION

Let us first describe circular polarization of a gravitational wave background. We use a plane wave expansion of the background as [8, 9]

$$h_{ij}(t, \mathbf{x}) = \sum_{P=+, \times} \int_{-\infty}^{\infty} df \int_{S^2} d\mathbf{n} h_P(f, \mathbf{n}) e^{2\pi i f(-t + \mathbf{n} \cdot \mathbf{x})} e_{ij}^P(\mathbf{n}). \quad (1)$$

Here, the amplitude h_P is the mode coefficient that is stochastic and random variable. The bases for transverse-traceless tensor \mathbf{e}^P ($P = +, \times$) are given as $\mathbf{e}^+ = \hat{\mathbf{e}}_\theta \otimes \hat{\mathbf{e}}_\theta - \hat{\mathbf{e}}_\phi \otimes \hat{\mathbf{e}}_\phi$ and $\mathbf{e}^\times = \hat{\mathbf{e}}_\theta \otimes \hat{\mathbf{e}}_\phi + \hat{\mathbf{e}}_\phi \otimes \hat{\mathbf{e}}_\theta$ with unit vectors $\hat{\mathbf{e}}_\theta$ and $\hat{\mathbf{e}}_\phi$. These vectors are normal to the propagation direction \mathbf{n} , associated with a right-handed Cartesian coordinate as usual. As an alternative characterization, we can use the circular polarization bases $\mathbf{e}^R = (\mathbf{e}^+ + i\mathbf{e}^\times)/\sqrt{2}$ (right-handed mode) and $\mathbf{e}^L = (\mathbf{e}^+ - i\mathbf{e}^\times)/\sqrt{2}$ (left-handed mode) for the plane wave expansion (1). The corresponding amplitudes h_R and h_L are given by $h_R = (h_+ - i h_\times)/\sqrt{2}$ and $h_L = (h_+ + i h_\times)/\sqrt{2}$. The ensemble average of their amplitudes is classified as

$$\begin{pmatrix} \langle h_R(f, \mathbf{n}) h_R(f', \mathbf{n}')^* \rangle \\ \langle h_L(f, \mathbf{n}) h_L(f', \mathbf{n}')^* \rangle \end{pmatrix} = \frac{\delta \mathbf{n}, \mathbf{n}' \delta_{f, f'}}{4\pi} \begin{pmatrix} I(f, \mathbf{n}) + V(f, \mathbf{n}) \\ I(f, \mathbf{n}) - V(f, \mathbf{n}) \end{pmatrix} \quad (2)$$

with the functions $\delta_{Y,Z}$ being delta functions. In the above expression, the real function V characterizes the asymmetry between the amplitudes of right- and the left-handed waves, while the function $I(\geq |V|)$ represents their total amplitude. Note that the other combinations such as $\langle h_R h_L^* \rangle$ and $\langle h_L h_R^* \rangle$ describe the linear polarization mode and are proportional to $Q \pm iU$, which constitute the well-known Stokes parameter, together with the I - and V - modes (see e.g., [10] for electromagnetic counterpart). In this paper, we do not study the linear polarization $Q \pm iU$, since they do not have an isotropic component. We will focus on the detectability of the isotropic components $I(f)$ and $V(f)$ as our primary target. Using the normalized logarithmic energy density of the background $\Omega_{\text{GW}}(f)$ [8, 9], the two functions I and V are expressed as

$$I(f) = \frac{\rho_c}{4\pi f^3} \Omega_{\text{GW}}(f), \quad V(f) = \frac{\rho_c}{4\pi f^3} \Omega_{\text{GW}}(f) \Pi(f), \quad (3)$$

where ρ_c is the critical density of the Universe, $\rho_c = 3H_0^2/8\pi$ with $H_0 = 70h_{70}$ km/sec/Mpc being the Hubble parameter. The ratio $\Pi(f) = V(f)/I(f)$ characterizes the circular polarization degree. For simplicity, we assume the flat spectra, $\Omega_{\text{GW}}(f) \propto f^0$ and $\Pi(f) \propto f^0$ as our fiducial model. Thus, our main interest is the simultaneous determinations or constraints on the parameters Ω_{GW} and Π .

We next consider how to detect the isotropic components of I - and V -modes with laser interferometers. Let us recall that the output signal s_a of a detector a at the position \mathbf{x}_a is written as $s_a(f) = \sum_{P=+,\times} \int_{S^2} d\mathbf{n} h_P(f, \mathbf{n}) F_a^P(\mathbf{n}, f) e^{i2\pi f \mathbf{n} \cdot \mathbf{x}_a}$. Here, the function F_a^P is the beam pattern function and it represents the response of the detector to a polarization mode e^P . Provided the data streams s_a and s_b taken from two detectors a and b , the detection of stochastic signals can be achieved by taking a cross-correlation, $\langle s_a(f) s_b(f')^* \rangle \equiv C_{ab}(f) \delta_{f,f'}$. Keeping the signals from the isotropic components, the correlation signal $C_{ab}(f)$ is written as

$$C_{ab}(f) = \gamma_{I,ab}(f) I(f) + \gamma_{V,ab}(f) V(f), \quad (4)$$

where the quantity γ_I is the overlap function given by [8, 9]

$$\gamma_{I,ab}(f) = \frac{5}{8\pi} \int_{S^2} d\mathbf{n} [\{F_a^+ F_b^{+*} + F_a^\times F_b^{\times*}\} e^{iy \mathbf{n} \cdot \mathbf{m}}], \quad (5)$$

with $y \equiv 2\pi f D/c$. Here, we have expressed $\mathbf{x}_a - \mathbf{x}_b$ as $D\mathbf{m}$ (D : distance, \mathbf{m} : unit vector). Similarly, the function $\gamma_{V,ab}(f)$ is obtained by replacing the kernel $[\dots]$ in Eq. (5) with $[i\{F_a^+ F_b^{\times*} - F_a^\times F_b^{+*}\} e^{iy \mathbf{n} \cdot \mathbf{m}}]$.

III. OVERLAP FUNCTIONS FOR GROUND BASED DETECTORS

Now, specifically consider the response of an L-shaped interferometer a on the Earth. We assume that the detector has two orthogonal arms with equal arm-length. Denoting the unit vectors parallel to the two arms by \mathbf{u} and \mathbf{v} , the beam pattern function takes a simple form as $F_a^P = \mathbf{d}_a : \mathbf{e}^P(\mathbf{n})$ with $\mathbf{d}_a = (\mathbf{u} \otimes \mathbf{u} - \mathbf{v} \otimes \mathbf{v})/2$, where the colon represents a double contraction. This expression is always valid as long as the wavelength of the gravitational waves for our interest is much longer than the arm-length of the detectors. In this paper we study the following five ongoing (and planned) kilometer-size interferometers as concrete examples; AIGO(A), LCGT(C), LIGO-Hanford(H), LIGO-Livingston(L) and Virgo(V) (see e.g. [11] for their basic information). Hereafter, we mainly use their abbreviations (A,C,H,L,V).

For the isotropic component of the stochastic background, only the relative configuration of two detectors is relevant with the correlation signal C_{ab} and we do not care about the overall rotation. Hence, the sensitivity of each pair of detectors to the stochastic background can be characterized by the three angular parameters $(\beta, \sigma_1, \sigma_2)$ shown in Fig. 1. Here, β is the separation angle between two detectors measured from the center of the Earth. The angle σ_1 (σ_2) is the orientation of the bisector of two arms of detector a (b) measured in counter-clockwise manner relative to the great circle connecting a and b . Their distance is given by $D = 2R_E \sin(\beta/2)$ ($R_E = 6400$ km : the radius of the Earth), which determines a characteristic frequency $f_D \equiv c/(2\pi D)$ for the overlap functions. Following Ref.[8], we define the angles

$$\Delta \equiv (\sigma_1 + \sigma_2)/2, \quad \delta \equiv (\sigma_1 - \sigma_2)/2. \quad (6)$$

The geometrical information about pairs of detectors among the five interferometers is presented in Table I.

In the expression (5), the angular integral can be performed analytically with explicit forms of the pattern functions. A long but straightforward calculation leads to [8]

$$\gamma_{I,ab} = \Theta_1(y, \beta) \cos(4\delta) + \Theta_2(y, \beta) \cos(4\Delta), \quad (7)$$

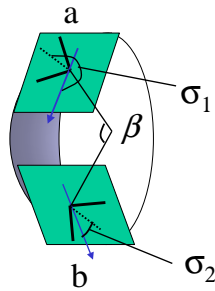


FIG. 1: Geometrical configuration of ground-based detectors a and b for the cross-correlation analysis. Detector planes are tangential to the Earth. Two detectors a and b are separated by the angle β measured from the center of the Earth. The angles σ_1 and σ_2 describe the orientation of bisectors of interferometers in a counter-clockwise manner relative to the great circle joining two sites.

	A	C	H	L	V
A	*	70.8°, -0.61	135.6°, -0.82	157.3°, -0.88	121.4°, 0.23
C	-0.58, 0.81	*	72.4°, 1.00	99.2°, -0.98	86.6°, -0.43
H	-1.00, -0.007	-0.21, 0.98	*	27.2°, -1.00	79.6°, -0.43
L	0.99, 0.15	0.04, -1.00	-0.36, -0.93	*	76.8°, -0.29
V	-0.45, -0.89	0.92, 0.38	-0.76, -0.65	0.89, -0.46	*

TABLE I: Upper right $(\beta, \cos(4\delta))$. Lower left $(\cos(4\Delta), \sin(4\Delta))$.

with $\Theta_1(y, \beta) = \cos^4\left(\frac{\beta}{2}\right) \left(j_0 + \frac{5}{7}j_2 + \frac{3}{112}j_4\right)$, and $\Theta_2(y, \beta) = \left(-\frac{3}{8}j_0 + \frac{45}{56}j_2 - \frac{169}{896}j_4\right) + \left(\frac{1}{2}j_0 - \frac{5}{7}j_2 - \frac{27}{224}j_4\right) \cos\beta + \left(-\frac{1}{8}j_0 - \frac{5}{56}j_2 - \frac{3}{896}j_4\right) \cos(2\beta)$. The function j_n is the n -th spherical Bessel function with its argument $y = f/f_D$. [8]. On the other hand, the overlap function for the V -mode is given by

$$\gamma_{V,ab} = \Theta_3(y, \beta) \sin(4\Delta) \quad (8)$$

with $\Theta_3(y, \beta) = -\sin\left(\frac{\beta}{2}\right) \left[(-j_1 + \frac{7}{8}j_3) + (j_1 + \frac{3}{8}j_3) \cos\beta\right]$. In Fig. 2, the overlap functions for the two representative pairs are shown in top (HL) and middle (CL) panels.

Here, we give a simple interpretation for the angular dependence of Eqs. (7) and (8). The beam pattern functions F_a^P and F_b^P are given by linear combinations of $(\cos(2\sigma_1), \sin(2\sigma_1))$ and $(\cos(2\sigma_2), \sin(2\sigma_2))$ respectively, reflecting their spin-2 like nature. Then, with Eq. (5) and addition formulas of trigonometric functions, the overlap functions should be linear combinations of $\cos[2(\sigma_1 \pm \sigma_2)]$ and $\sin[2(\sigma_1 \pm \sigma_2)]$, namely, $\cos(4\Delta)$, $\cos(4\delta)$, $\sin(4\Delta)$ and $\sin(4\delta)$. Since the expectation value $C_{ab}(f)$ is a real function for our beam pattern functions, we have $\langle s_a s_b^* \rangle = \langle s_b s_a^* \rangle$. This essentially results in replacing the roles of σ_1 and σ_2 , and the functions γ_I and γ_V cannot contain terms proportional to $\sin(4\delta) = \sin[2(\sigma_1 - \sigma_2)]$.

On the other hand, while the observable $C_{ab}(f)$ and the amplitude I are invariant under the parity transformation of a coordinate system, the sign of the parameter V flips, because the transformation interchanges right- and left-handed waves. Therefore, the function $\gamma_{V,ab}$ must change its sign while keeping the quantity $C_{ab}(f)$ invariant. Geometrically, this corresponds to the re-definition of the azimuthal angles $\sigma_{1,2}$ in a clockwise direction (or putting $\sigma_1 \rightarrow -\sigma_1$ and $\sigma_2 \rightarrow -\sigma_2$). As a result, the function $\gamma_{V,ab}$ should be odd functions of δ and Δ , and it must be proportional to $\sin(4\Delta)$ as shown in Eq. (8) (the term proportional to $\sin(4\delta)$ is already prohibited as explained earlier). With similar arguments, we find that the function γ_I is a linear combination of $\cos(4\Delta)$ and $\cos(4\delta)$ as in Eq. (7).

A. Special cases

To stress the importance of the geometric configuration, it is instructive to consider several simple examples for idealistic pair of detectors. When a pair of detectors is co-located ($\beta = 0^\circ$ and $D = 0$), the functions (Θ_1, Θ_2) defined after Eq. (7) become $(1, 0)$ and we have $\gamma_{I,ab} = \cos(4\delta)$. The identity $\Theta_2 = 0$ at $\beta = 0^\circ$ implies that the function

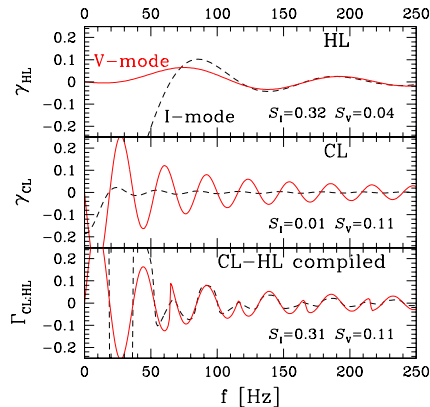


FIG. 2: Overlap functions for the un-polarized I mode (dashed curves), and the circularly polarized V -mode (solid curves). The upper panel shows the results for the Hanford-Livingston (HL) pair (the characteristic frequency $f_D = 100\text{Hz}$). The middle one is results for the LCGT-Livingston (CL) pair ($f_D = 31\text{Hz}$). The normalized SNRs $S_{I,V}$ (with the adv LIGO noise spectrum) are also presented. The bottom one show the compiled functions $\Gamma_{I,V}$ (eq.(10)) made from both pairs.

γ_I depends very weakly on the parameter Δ at a small angle $\beta \sim 0^\circ$. On the other hand, the overlap function $\gamma_{V,ab}$ always vanishes for a pair of detectors in the same plane ($\beta = 0$). This is even true with a finite separation $D \neq 0$. This exact cancellation comes from the geometric symmetry of the beam pattern function with respect to the detector plane [7, 12].

For two detectors at antipodal positions ($\beta = 180^\circ$), we have $\Theta_1 = 0$ and the angle δ becomes geometrically meaningless. One can expect that the function $\gamma_{I,ab}$ is almost proportional to $\cos(4\Delta)$ near $\beta = 180^\circ$.

B. Broadband SNR

Now, we turn to focus on a broadband sensitivity to the I - and V -modes. In the weak signal limit, the total signal-to-noise ratio (SNR) for the correlation signal $C_{ab}(f)$ is given by [8]

$$\text{SNR}^2 = \left(\frac{3H_0^2}{10\pi^2} \right)^2 T_{\text{obs}} \left[2 \int_0^\infty df \frac{X^2}{f^6 N_a(f) N_b(f)} \right] \quad (9)$$

with $X = \gamma_I \Omega_{\text{GW}} + \gamma_V \Omega_{\text{GW}} \Pi$. We denote the noise spectra for detectors a and b by $N_a(f)$ and $N_b(f)$, assuming no noise correlation between them. In what follows, for simplicity of our analysis, we further assume that all the detectors have the same sensitivity comparable to the noise spectral curves of advanced LIGO. The analytical fit from Fig. 1 of Ref.[2] leads to $N(f) = 10^{-44} (f/10\text{Hz})^{-4} + 10^{-47.25} (f/10^2\text{Hz})^{-1.7} \text{Hz}^{-1}$ for $10 \text{Hz} \leq f \leq 240 \text{Hz}$, $N(f) = 10^{-46} (f/10^3\text{Hz})^3 \text{Hz}^{-1}$ for $240 \text{Hz} \leq f \leq 3,000 \text{Hz}$, and otherwise $N(f) = \infty$. Note that the combination $f^6 N(f)^2$ becomes minimum around $f \sim 50\text{Hz}$ with its bandwidth $\Delta f \sim 100\text{Hz}$. For a pair of coincident detectors (i.e., $\gamma_{I,ab} = 1$ and $\gamma_{V,ab} = 0$), the total SNR is evaluated by setting $X = \Omega_{\text{GW}}$ in Eq. (9), and we numerically obtain $\text{SNR}_0 = 4.8 (T_{\text{obs}}/3\text{yr})^{1/2} (\Omega_{\text{GW}} h_{70}^2/10^{-9})$.

The total SNR depends strongly on model parameters of the background, including the polarization degree Π . In order to present our numerical results concisely, we first calculate $\text{SNR}_{\{I,V\},ab}$ by plugging $X = \gamma_{\{I,V\},ab}$ into Eq. (9) and then normalize them as $S_{\{I,V\},ab} \equiv \text{SNR}_{\{I,V\},ab}/\text{SNR}_0$. The normalized SNRs can be regarded as rms values of $\gamma_{\{I,V\},ab}$ with a weight function $[f^6 N(f)^2]^{-1}$.

C. Optimal configuration

Let us discuss optimal configurations of two detectors (a, b) for measuring the I - and V -modes with the correlation signal C_{ab} . There are two relevant issues here: maximization of the signals $S_{I,ab}$ and $S_{V,ab}$, and switching off either of them ($S_{I,ab} = 0$ or $S_{V,ab} = 0$) for their decomposition. To deal with the situation comprehensively, we consider how to

set the second detector b relative to the fixed first one a with a given separation angle β . In this case, the sensitivity to the I - and V -modes is characterized by the remaining adjustable parameters, σ_1 and σ_2 . The former determines the position of the detector b , while the latter specifies its orientation (see Fig. 1). Based on the expressions (7) and (8), one finds that there are three possibilities for the optimal detector orientation: $\cos(4\Delta) = -\cos(4\delta) = \pm 1$ (type I) or $\cos(4\Delta) = \cos(4\delta) = \pm 1$ (type II) to maximize the normalized SNR $S_{I,ab}$ [8], and $\cos(4\Delta) = \cos(4\delta) = 0$ (type III) to erase the contribution from I -mode. For type I, the solutions of the two angles $\sigma_{1,2}$ are $\sigma_1 = \sigma_2 = 45^\circ$ (mod 90°) and the detector b must be sited in one of the two great circles passing through the detector a , parallel to one of the two arms. For type II, the second detector must reside in two great circles parallel or perpendicular to the bisecting line of each detector. Similarly, the type III configuration is realized by placing the second detector on one of the four great circles defined for types I and II, with rotating 45° relative to the first detector.

Note that the sensitivity to the V -mode is automatically switched off for the type I and II configurations and is conversely maximized for the type III configuration. This is because the normalized SNR $S_{V,ab}$ is proportional to $\sin(4\Delta)$. While a definite detection of a weak V -mode signal requires a careful removal of the I -mode signal from observed data, it turns out that the geometrical requirement for type III configuration is severe. As we see later, however, we can easily control the contribution from the I - (or V -)mode by introducing a third detector.

In Fig. 3, we present the normalized SNRs for the optimal geometries; types I, II and III (short-dashed, long-dashed, and solid curves, respectively). One noticeable point is that a widely separated ($\beta \sim 180^\circ$) pair is powerful to search for the V -mode (recall the cancellation $\gamma_V = 0$ at $\beta = 0$). To reduce the contribution from the I -mode, pairs that are usually disadvantageous to measuring the total intensity Ω_{GW} now play a very important role. In Fig. 3, we also show the normalized SNRs for representative pairs made from the five detectors, in which several interesting combinations are found. The HL (with $\cos(4\delta) \sim 1$ and $\sin(4\Delta) \sim 0.93$) realizes nearly maximum values simultaneously for $S_{I,ab}$ and $S_{V,ab}$ at its separation $\beta = 27.2^\circ$. This is because $S_{I,ab}$ is mainly determined by the angle δ at a small β , while $S_{V,ab}$ depends only on Δ . The CL has good sensitivity to the V -mode and relatively insensitive to the I -mode with $\sin(4\Delta) \sim 1$. In contrast, AH is almost insensitive to the V mode with $\sin 4\Delta = -0.007$. In this sense, LCGT and AIGO detectors are suitably oriented to probe the I - and V -modes, respectively.

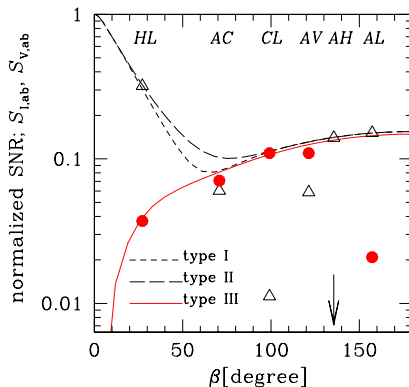


FIG. 3: Normalized signal to noise ratios ($S_{I,ab}$ and $S_{V,ab}$) with optimal configurations for the I -mode (short dashed curve: type I, long dashed curve: type II) and for the V -mode (solid curve: type III with setting $\Pi = 1$ for illustrative purpose). We use the noise curve for the advanced LIGO. For each detector pair, S_I and S_V are given with a triangle and a circle respectively at its separation β . There are four other pairs not shown here; CH with $(S_I, S_V) = (0.04, 0.08)$, LV with $(0.08, 0.04)$, HV with $(0.07, 0.06)$ and CV with $(0.09, 0.04)$.

D. Separating I - and V -modes

As a final mention, we will address the issue of I - and V -mode separation by combining several pairs of detectors. For preliminary investigation, we consider the case that two pairs of interferometers (a, b) and (c, d) are available. Detectors a and c can be identical, but we need at least three independent detectors for the study below. First note that the correlation signals are given by $C_{ab}(f) = \gamma_{I,ab}(f) I(f) + \gamma_{V,ab}(f) V(f)$ and $C_{cd}(f) = \gamma_{I,cd}(f) I(f) + \gamma_{V,cd}(f) V(f)$. From this, one can easily find that the contribution from the I -mode is canceled by taking a combination $W \equiv \gamma_{I,ab} C_{cd} - \gamma_{I,cd} C_{ab} = (\gamma_{V,cd} \gamma_{I,ab} - \gamma_{V,ab} \gamma_{I,cd}) V(f)$. The statistical analysis based on the combination W would be

a robust approach for actual V -mode search, although a further refinement may be possible by combining more pairs, which we will report elsewhere.

Since the rms amplitude of the detector noise for the combination W becomes $N(f) (\gamma_{I,ab}^2 + \gamma_{I,cd}^2)^{1/2}$, we define the *compiled* overlap function for the V mode by

$$\Gamma_{V,ab:cd} \equiv \frac{\gamma_{V,cd}\gamma_{I,ab} - \gamma_{V,ab}\gamma_{I,cd}}{[\gamma_{I,ab}^2 + \gamma_{I,cd}^2]^{1/2}}. \quad (10)$$

This expression should be used in Eq. (9) when evaluating the broadband SNR for the V -mode with the combination W . In a similar way, we define the compiled function $\Gamma_{I,ab:cd}$ for the I mode by interchanging the subscripts V and I in Eq. (10). Bottom panel of Fig. 2 shows the compiled overlap functions $\Gamma_{\{I,V\},ab:cd}$ from two pairs of detectors, CL-HL. With this combination, the normalized SNR becomes 0.11 for the V -mode and 0.31 for the I -mode. Using numerical results below eq.(9), the detection limit for the polarization degree Π is given as $\Pi = (T/3\text{yr})^{-1/2}(SNR_V/5)(\Omega_{\text{GW}}h_{70}^2/10^{-8})^{-1}$ with signal-to-noise ratio SNR_V . These numerical results are almost the same values as in S_V for CL and S_I for HL, and in this sense, the I -, V -mode separation can be performed efficiently with naively expected sensitivities $S_{\{I,V\},ab}$. Note that the other combinations, such as AV-HL, AV-HV and CL-HV, also provide the normalized value ~ 0.11 for the V -mode, but AH-AL has only 0.015.

In summary, we reported principle aspects for measuring a circular polarization degree of a gravitational wave background that is related to parity violation. We find that pairs of ground-based interferometers that are widely separated and relatively insensitive to the total intensity Ω_{GW} are advantageous for the measurement. With at least three detectors, the polarization degree and the intensity Ω_{GW} can be separately detected.

We would like to thank N. Kanda and M. Ando for supplying information on LCGT and comments. This work was supported in part by a Grant-in-Aid for Scientific Research from the Japan Society for the Promotion of Science (No. 18740132).

-
- [1] B. Abbott et al. Phys. Rev. Lett. **95**, 221101 (2005).
 - [2] E. Gustafson et al. 1999, LIGO project document T990080-00-D.
 - [3] K. Kuroda *et al.* Int. J. Mod. Phys. D **8**, 557 (1999).
 - [4] S. H. S. Alexander et al. Phys. Rev. Lett. **96**, 081301 (2006); M. Satoh, S. Kanno and J. Soda, arXiv:0706.3585 [astro-ph].
 - [5] A. Lue, L. M. Wang and M. Kamionkowski, Phys. Rev. Lett. **83**, 1506 (1999).
 - [6] C. Caprini, R. Durrer and T. Kahniashvili, Phys. Rev. D **69**, 063006 (2004); S. Saito, K. Ichiki and A. Taruya, arXiv:0705.3701 [astro-ph].
 - [7] N. Seto, Phys. Rev. Lett. **97**, 151101 (2006); Phys.Rev.D **75**, 0601302 (2007).
 - [8] E. E. Flanagan, Phys. Rev. D **48**, 2389 (1993).
 - [9] B. Allen and J. D. Romano, Phys. Rev. D **59**, 102001 (1999).
 - [10] G. B. Rybicki and A. P. Lightman, *Radiative Process in Astrophysics* (Wiley, New York, 1979).
 - [11] N. Arnaud et al. Phys.Rev.D **65**, 042004 (2002).
 - [12] H. Kudoh and A. Taruya, Phys. Rev. D **71**, 024025 (2005).